Evidence from Climate Models for a Role of ENSO Events in Shaping the Climatological Size and Temperature of the Warm-pool

Yan Sun[1,2], De-Zheng Sun*[2], and Lixin Wu[1],

[1] Physical Oceanography Laboratory/College of Physical and Environmental Oceanography, Ocean University of China, Qingdao, China

[2] Cooperative Institute for Research in Environmental Sciences, University of Colorado, and NOAA/Earth System Research Laboratory/Physical Sciences Division, Boulder, Colorado, USA

September 16, 2011

Submitted to J. Climate

* Corresponding author: Dr. De-Zheng Sun, Cooperative Institute for Research in Environmental Sciences, University of Colorado, and NOAA/Earth System Research Laboratory/Physical Sciences Division, Boulder, Colorado, USA. Email: dezheng.sun@noaa.gov

Abstract

Theory and empirical studies have suggested that an underestimate of the ENSO asymmetry may result in a climatologically smaller and warmer western Pacific warm-pool. Simulations of the tropical Pacific climate by 19 IPCC AR4 climate models that do not use flux adjustment are evaluated in light of this suggestion. The evaluation reveals systematic biases in both the mean state as well as in the ENSO statistics. It is found that the mean state in most of the models has a smaller and warmer warm pool. This common bias in the mean state is accompanied by a common bias in the simulated ENSO statistics: a significantly weak asymmetry between the two phases of ENSO. These findings add support for the suggested impact of ENSO asymmetry on the tropical mean state—the climatological size and temperature of the warm-pool in particular. More importantly, together with previous studies, the findings light up a path to improve the simulation of the tropical Pacific mean state by climate models: enhancing the asymmetry of ENSO in the climate models.

1. Introduction

While fundamentally no region in the Earth's climate system deserves special attention, the Western Pacific warm-pool does have one unique aspect: it has the highest SST in the world's open oceans (Newell 1979, Ramanathan and Collins 1991). As we are increasingly concerned with whether we have reached "the point of no-return" for the earth's climate system (Hansen et al. 2008), we have good reasons to be especially concerned with our models' performance in simulating the warmest region on the Earth.

The western Pacific warm pool (here after we simply refer to as the warm-pool) has been also been referred to as a major furnace of the Earth's climate system (Pierrehumbert 1995). This is because that it is the region where tropical deep convection is concentrated and the latent heat release reaches a broad maximum (Spencer 1993). The latent heat release powers the Walker and Hadley circulation in the atmosphere, which in turn drives the currents in the upper ocean (Sun and Liu 1996; Djikstra and Neelin 1995; Trenberth and Solomon 1994; Webster and Lukas 1992; Philander 1990; Held and Hou 1980). The atmospheric Hadley circulation and its counterpart in the ocean: the meridional branch of the wind-driven circulation extends the influence of the warm pool to the extratropical region (Held and Hou

1980, Sun and Lindzen 1994; Hou 1998; Lu et al. 1998, McPhaden et al. 1998). This critical role of the warm pool in the dynamics of the climate system gives additional reason to know how well our state-of-the-art climate models simulate the major characteristics of the warm pool.

Some previous studies have reported some biases in the mean state of the warm pool in the coupled climate models. The earliest study using outputs from multiple models is probably the seminal one by Mechoso et al. (1995). They noted that an excessive cold-tongue was a common feature among the models they examined, implying the zonal extend of the warm pool in the models may be too confined to the west. Kiehl (1998) directly examined the warm pool simulation by CCSM1 (Kiehl et al. 1998; Boville and Gent 1998) and found the same bias as seen in Mechoso et al. (1995) in other models. Kiehl (1998) hypothesized that the excessive solar heating reaching the warm-pool may force a stronger zonal winds and therefore an extended cold-tongue (or a smaller warm-pool). These studies, however, examined only a single run of the concerned models. As the observation is a single realization, it is important to examine the spread of the ensemble runs to draw a conclusion with confidence about the biases in the models.

Wee attempt to evaluate the simulations by the climate models in IPCC AR4 of the warm-pool in a more thorough way. We will not only examine a large set of models—we will examine all of the no flux adjustment IPCC AR4 models, but also the available ensemble runs of individual models. These outputs allow us to construct

PDFs using the largest data set available and put the estimate of bias on a stronger statistical footing than studies that are limited to a single model, or to a single run of multiple models.

The main motivation for this study, however, is to check whether recent theoretical and empirical predictions regarding a role of ENSO events in determining the mean state of the warm-pool is indeed supported by, or at least consistent with the results from models. Specifically, theoretical and empirical studies have suggested that if models underestimate the nonlinearity in the ENSO dynamics, then the size of the warm-pool should be smaller, and the mean warm pool SST is greater than the observations (Rodgers et al. 2004, Schopf and Burgman 2006, Sun and Yu 2009, Sun and Zhang 2006, Sun 2010). We will check whether the simulations by the climate models collected by IPCC AR4 (Meehl et al. 2007) support or contradict these empirical and theoretical findings. We want to check whether the way the time mean state of the warm-pool is biased and the way ENSO is biased in the models have a relationship that is consistent with what is implied by the aforementioned empirical and theoretical results. For this purpose, we also attempt to evaluate the simulations by the climate models in IPCC AR4 of ENSO statistics (ENSO asymmetry in particular) in a more thorough way than previous studies: we will evaluate the statistics of ENSO events in the same aforementioned manner to evaluate the climatological size and temperature of the warm-pool. Many studies have evaluated ENSO asymmetry in climate models before (An et al. 2009, Zhang et al. 2009, and Sun 2010). However, similar to the previous studies that have examined the climatology of the warm-pool, these studies of evaluating ENSO asymmetry examined only a single run of the concerted models. The number of the models examined is also more limited. For example, the study by An et al. (2005) employed 10 models. The study of Zhang et al. (2009) and Sun (2010) focused on the NCAR CCSMs (the early versions of CESM; see http://www.cesm.ucar.edu/).

The collective effect of ENSO events on the mean Pacific climate in general and on the warm pool in particular was first suggested from the asymmetry between its warm phase (El Niño) and cold phase (La Niña)—the sum of the two does not cancel but has a spatial pattern resembling the anomaly in the warm phase (Burgers and Stephenson 1999, Rodgers et al. 2004, Sun and Yu 2009). This effect has been referred as the residual of ENSO in these and related studies. Attempting to address the question of the time-mean effect of ENSO events more rigorously, Sun and Zhang (2006) employed a hybrid model—an empirical atmosphere coupled with an Ocean GCM—to contrast the response of the tropical Pacific mean climate to a perturbation in the presence of ENSO events with a case in which ENSO events are surgically suppressed. From the results, they found that ENSO events tend to cool the center of the western Pacific warm pool and warm the central Pacific, thus effectively extend the size of the warm pool but reducing the maximum SST. Sun (2010) further reported some preliminary results from forced ocean model experiments in which the strength of the ENSO fluctuations in the surface winds are varied. The preliminary results seem to confirm the findings of Sun and Zhang (2006).

The paper is organized as follows. Information about the models and the data sets is provided in section 2. The results about the biases in the climatological state of the warm-pool and ENSO statistics are presented in Section 3. Summary and conclusion are provided in section 4.

2. Data and Methodology

2.1 Observations

The observational SST data used in this study is the Hadley Centre sea ice and sea surface temperature data set Version 1 (HadISST1, Rayner et al. 2003). It has been developed at the Met Office Hadley Centre, and the monthly data are available from 1871 to present. The SST field is built from in-situ and satellite observations and is given on a 1^{o}x1^{o} grid. Data used in this study cover the period from January 1900 to December 1999.

2.2 Models

The model data are the 20c3m scenario simulations by climate models in IPCC AR4 (ftp-esg.ucllnl.org (Meehl et al. 2007)). The analysis is limited to the no flux adjustment models. The 19 no flux adjustment models, together with the numbers of runs each individual models have in the IPCC AR4, are listed in Figure 1. All together, 53 models runs are used in our construction of the statistics of the warm-pool climatology and ENSO characteristics. The descriptions of all the models listed can be obtained from this website http://www-pcmdi.llnl.gov/ipcc/model_documentation/ipcc_model_documentation.php. The whole 20th century (January 1900 to December 1999) has been employed for the analysis, though we will focus on presenting the results of the last 50 years in the present paper, as the observational data are more reliable during this latter period.

3. Results

The multi-model ensemble runs allow us to construct a probability density function (PDF) for the warm-pool size. It is shown as the blue curve in Figure 2. The vertical line in blue indicates the multi-model ensemble mean value--the averaged warm pool size simulated by all model runs. The red line indicates the observed value. The short colored bars on the horizontal axis mark the ensemble mean value of the warm-pool size of each model. Figure 2 shows that most of the model runs have a warm-pool size that is smaller than the observations. Measured by the ensemble mean value of each model, ¾ of the models underestimate the size of the warm-pool. The multi-model ensemble mean value of the warm-pool size is only about 80% of the size of the observed warm-pool (Figure 2a). The PDF is also obviously negatively skewed, suggesting that it is more difficult to increase the size of the warm-pool in the models than to decrease it.

Figure 2b further shows the time series of the ensemble mean value of the warm-pool size simulated by each model over the entire period where model runs are available. The figure shows that the majority models that are identified to underestimate the size of the warm-pool size do so throughout the entire century.

(The few models that are identified in Figure 2a that have a larger warm-pool than in the observations do so also throughout the entire period). Redoing Figure 2a using different periods of data show that the underestimate of the warm pool size does not depend on whether the data are from the whole 20th century, the last 50 years or the last 30 years in the 20th century are used in the construction of the PDF.

A major contributor to the smaller warm pool size in the models is that most of the models continue to have an excessive westward extension of the cold tongue (Figure 3). The figure shows the time-mean position of the 28^{o}C SST from the models and the observations. The ensemble mean SST from each model is used to obtain this figure. Another contributor to the smaller size of the warm-pool is that the main part of the warm-pool (west of 160^{o}E) in the models is more confined meridionally to the equator, particularly in the north hemisphere (Figure 3).

The spread of the warm-pool size from different runs in the same model are found small relative to their differences with the observations. An example is given in Figure 4 which shows the warm pool size simulated by all the runs of the same model--the NCAR CCSM3 (a) and GFDL CM2.1 (b). The results suggest that the intrinsic errors in individual models are responsible for the model-observation discrepancies.

Although the size of the warm-pool in the models is generally smaller than that in the observations, the warm-pool in the models is warmer than that in the observations, measured either by the mean SST over the warm-pool (Figure 5) or its maximum SST (Figure 6). Figure 5 (6) a, b are respectively the same as Figure 2a,b except they are for the mean SST of the warm-pool (Figure 5) and for the maximum SST (Figure 6). The time series of these quantities (Figure 5b and Figure 6b) show that these discrepancies between the model simulations and observations remain relatively constant in the entire period of the simulations. The model-observation discrepancies in the maximum SST are particularly striking given that in the observations, the maximum SST is almost always around 30ºC –the variability is within 0.5 ºC over the entire century. The maximum SST in models, in contrast, spreads from 27ºC to 35ºC in comparison. 12 of the 19 models simulate a higher maximum SST. The averaged maximum SST over the tropical Indo-Pacific of all model runs is 30.85ºC, which is about 0.4ºC higher than in the observation (30.44ºC, Figure 6a). Also note that the PDF for the maximum SST is highly positively skewed, suggesting that in the models, it is easier to increase the maximum SST then decreasing it.

3.1 ENSO asymmetry in the models.

Using multi-model ensemble runs, we have uncovered a common bias in the models: the warm-pool in the models is generally smaller and warmer than in the observations. This standing-out bias provides an opportunity to test the theoretical and empirical predictions about the nonlinear rectification effect of ENSO activity into the climatological size and temperature of the warm-pool. If the simulated ENSO statistics does have a distinct bias, and the bias is in the direction that would cause the bias we have already uncovered in the climatology of the warm-pool in the manner suggested by the aforementioned empirical studies, our suspicion of a nonlinear rectification effect of ENSO on the mean state will be enhanced. Towards this end, we have also evaluated ENSO statistics in the models, in particular, the ENSO asymmetry as it is a measure of the nonlinearity of ENSO dynamics and therefore the time-mean effect of ENSO events (Sun and Zhang 2006; Schopf and Burgman 2006).

A typical way to measure ENSO asymmetry is the skewness of Nino3 SST (Burgers and Stephenson 1999; An et al. 2005). A PDF is constructed for the skewness of the Nino3 SST in the models and observations in the same way as for the warm-pool size and temperature. This PDF is shown in Figure 7. (The same multi-model ensemble runs are used for Figure 7 and Figure 2a.). The figure reveals that models generally underestimate the ENSO asymmetry. Skewness of Niño3 SST anomaly in observation is positive (redline in Figure 7) in contrast with the negative ones in most of the model runs. Some model runs have positive skewness, but none of them reach the observed value. The skewness of Nino3 SST anomaly from observations is 0.88 based on the 50 year data from 1950-1999. The minimum skewness of ENSO anomalies in the model runs is -0.60 and the maximum one is 0.44. The averaged skewness of Niño3 SST anomaly in all model runs is close to zero, indicating a near symmetric ENSO in the no flux adjustment IPCC models (Figure 7).

To show this common model bias in a more traditional method, we have also plotted the histogram of the Nino3 SST anomaly distribution (Figure 8). The symmetric nature of ENSO in the models can be readily seen from this figure. In the observations, the cooling events occurred more frequently than the warming events and the strongest cooling events are weaker than the strongest warm events. In contrast, there are equal occurrences of cooling and warming events in almost all the models. The modeled ENSO events are also much less asymmetric in magnitude than in the observations. The modeled ENSO asymmetry biases has been noted by Leloup et al (2008) and An et al. (2009) in a more limited set of climate models . Zhang et al. (2009) noted the underestimate of the ENSO asymmetry in the NCAR CCSM models and explored its courses by contrasting the differences among the successive versions of the NCAR CCSM (and now is called CESM).

The difference in the frequency distribution of Niño3 SST anomaly among different runs by the same model is also found small relative to their differences from the observations. Figure 9 shows the frequency distribution of monthly Niño3 SST anomaly simulated by all the runs of the same model--the GFDL models (Figure 9ab) and the NCAR models (Figure 9cd). This suggests that the intrinsic errors in individual models are responsible for the model-observation discrepancies.

3.3: Biases in the ENSO Asymmetry: A cause of a smaller and warmer *warm-pool?*

The weak ENSO asymmetry in the models may give us an explanation of the biases in the warm pool simulation in the models. As suggested by the aforementioned empirical as well as theoretical studies (Rodgers et al. 2004, Sun and Yu 2009, Schopf and Burgman 2006, Sun and Zhang 2006, Sun 2010), the time mean effect of ENSO in the observations is to cool the center of the warm-pool, and warm the central Pacific. In other words, it reduces the maximum SST of the warm pool and expands the size of the warm pool. Judging from the lack of the asymmetry in the modeled ENSO, such a time mean effect of ENSO is either too weak, or non-existent in the models, causing a warmer bias in the maximum SST of the warm pool, but a smaller size of the warm pool in the models.

4. Conclusions

Motivated by recent empirical as well as theoretical results concerning the time-mean effect of ENSO events on the tropical Pacific climatology, we have examined the biases in the simulations of the western Pacific warm-pool in relationship with the biases in the ENSO statistics. A common bias in the simulation of the warm pool is a smaller and warmer warm pool in the models than in the observations. A corresponding common bias in the simulation of ENSO is the lack of ENSO asymmetry. Such a correspondence cannot prove, but certainly does not contradict the empirical and theoretical prediction that the underestimate of ENSO asymmetry in most models may cause a smaller but warmer warm-pool. Given the many factors that can affect the simulation of the warm-pool and the diversity in the physical packages of the models, the chance of such a correspondence coming out of random is likely small. It follows that the suggested time-mean effect needs to be taken seriously, and that improving ENSO statistics—the ENSO asymmetry in particular-- could be an effective path to improving the simulation of the tropical Pacific climatology. It is also possible that the biases in the warm-pool climatology caused by a bias in the ENSO asymmetry may further enhance the bias in the ENSO asymmetry, causing an vicious cycle that is hard to break and thus explaining the persistence of the biases that have been noted in the two key aspects of the tropical Pacific climate. Fully recognizing this possibility, however, may help us to formulate a more complete strategy to improve the tropical Pacific climate on which climate variability over much of the world depend.

The importance of dynamical coupling in creating the climatological warm-pool and cold-tongue configuration in the tropical Pacific has been long recognized (Dijkstra and Neelin 1995, Sun and Liu 1996, Clement et al. 1996, and Jin 1996). The relative roles of clouds and ocean dynamics in creating and maintaining the western Pacific warm-pool have also been assessed (Clement et al. 2005). But these studies have not addressed the collective role of ENSO events from the scale-interaction prospective. Thus, the present study, together with those earlier ones in this line of thinking, extend our understanding of the maintenance of the warm pool by assessing the potential importance of rectification of ENSO events in shaping the size and temperature of the warm-pool.

Acknowledgements

This work was supported by Chinese Scholarship Council, the Ocean University of China, the Large-scale and Climate Dynamics Program of the US National Science Foundation (AGS 0553111 and AGS 0852329), the Major Project of National Science Foundation of China (Grant No: 40890150, 40890155), the National Science Foundation for Distinguished Young Scholars of China (Grant No: 40788002), the National Science Foundation Creative Research Group Project (Grant No: 40921004). All the data analysis work was carried on the computers at Physical Science Division of Earth System Research Laboratory of the National Oceanic and Atmospheric Administration. We would like to thank University of Colorado at Boulder for hosting Yan Sun. We would also like to thank Dr. Tao Zhang for his help on some programming issues.

References

An, Soon-Il, Yoo-Geun Ham, Jong-Seong Kug, Fei-Fei Jin, In-Sik Kang, 2005: El Niño–La Niña Asymmetry in the Coupled Model Intercomparison Project Simulations. *J. Climate*, **18**, 2617–2627.

Boville, B.A., and P.R. Gent, 1998: The NCAR Climate System Model, Version one. J. Climate, 11, 1115-1130. Burgers, G., and D.B. Stephenson 1999: The "Normality" of El Niño, Geophys. Res. Lett., 26, 1027-1030. Clement, Amy C., Richard Seager, Raghu Murtugudde, 2005: Why Are There Tropical Warm Pools? *J. Climate*, **18,** 5294–5311. doi: 10.1175/JCLI3582.1

Burgers, G., and D. B. Stephenson, 1999: The "normality" of El Niño. *Geophys. Res. Lett.*, **26,** 1027-1030, doi:10.1029/1999GL900161.

Clement, A. C., R. Seager, M. A. Cane and S. E. Zebiak, 1996: An ocean dynamical thermostat. *Journal of Climate*, **9**(9): 2190-2196.

Clement, A. C., R. Seager and R. Murtugudde, 2005: Why are there tropical warm pools? *Journal of Climate*, **18**(24): 5294-5311.

Dijkstra, H. A., and J. D. Neelin 1995: Ocean–atmosphere interaction and the tropical climatology Part II: Why the Pacific cold tongue is in the east, *J. Climate,* **8,** 1343–1359.

Hansen, J., Mki. Sato, P. Kharecha, D. Beerling, R. Berner, V. Masson-Delmotte, M. Pagani, M. Raymo, D.L. Royer, and J.C. Zachos, 2008: Target atmospheric CO_2: Where should humanity aim? *Open Atmos. Sci.* J., 2, 217-231, doi:10.2174/1874282300802010217.

Held, I. M., and A. Y. Hou 1980: Nonlinear axially symmetric circulations in a nearly inviscid atmosphere, *J. Atmos. Sci.,* **37,** 515–533.

Hou, A. Y. 1998: Hadley circulation as a modulator of the extratropical climate, *J. Atmos. Sci.,* **55,** 2437–2457.

Hou, A. Y. 1998: Hadley circulation as a modulator of the extratropical climate, *J. Atmos. Sci.,* **55**, 2437–2457.

Jin, F.-F., 1996: Tropical ocean interaction, Pacific cold tongue, and El Niño Southern Oscillation. *Science*, **274,** 76–78.

Kiehl, J. T. 1998: Simulation of the tropical Pacific warm-pool with the NCAR climate system model, *J. Climate,* **11,** 1342–1355.

Leloup, J., M. Lengaigne and J.-P. Boulanger 2008: Twentieth century ENSO characteristics in the IPCC database, *Clim. Dyn.,* **30,** 277-291.

Lu, P., J. P. McCreary Jr., and B. A. Klinger 1998: Meridional circulation cells and the source waters of the Pacific equatorial undercurrent, *J. Phys. Oceanogr.,* **28,** 62–84.

McPhaden MJ, and co-authors, 1998: The Tropical Ocean-Global Atmosphere observing system: A decade of progress. *J. Geophys. Res.,* **103(C7),** 14,169-14,240

Mechoso, M. R., and Coauthors 1995: The seasonal cycle over the tropical Pacific in coupled ocean–atmosphere general circulation models, *Mon. Wea. Rev.,* **123,** 2825–2838.

Meehl, G.A., C. Covey, T. Delworth, M. Latif, B. McAvaney, J.F.B. Mitchell, R.J. Stouffer and K.E. Taylor 2007: The WCRP CMIP3 Multimodel Dataset: A New Era in Climate Change Research, *BAMS*, **88,** 1383-1394, DOI: 10.1175/BAMS-88-9-1383.

Newell, R. E., 1979: Climate and the ocean. *Amer. Sci*., **67**, 405–416.

Philander, S. G. 1990: El Niño, La Niña and the Southern Oscillation, 293 pp, Elsevier, New York.

Pierrehumbert, R. T. 1995: Thermostats, radiator fins, and the runaway greenhouse, *J. Atmos. Sci.,* **52,** 1784–1806.

Ramanathan, V. and W. Collins 1991: Thermodynamic regulation of ocean warming by cirrus clouds deduced from observations of the 1987 El Niño. *Nature,* 27—32.

Rayner N. A., D. E. Parker, E. B. Horton, C. K. Folland, L. V. Alexander, D. P. Rowell, E. C. Kent, and A. Kaplan 2003: Global analyses of sea surface temperature, sea ice, and night marine air temperature since the late nineteenth century, *J. Geophys. Res.,* **108,** 4407, doi:10.1029/2002JD002670.

Rodgers, K. B., P. Friederichs, and M. Latif 2004: Tropical Pacific decadal variability and its relation to decadal modulation of ENSO, *J. Climate,* **17,** 3761–3774.

Schopf, P. S., and R. J. Burgman 2006: A simple mechanism for ENSO residuals and Asymmetry, *J. Climate,* **19,** 3167–3179.

Spencer, R. W. 1993: Global oceanic precipitation from the MSU during 1979-91 and comparisons to other climatologies, *J. Climate,* **6,** 1301-1326.

Sun, D.-Z. 2003: A possible effect of an increase in the warm-pool SST on the magnitude of El Niño warming, *J. Clim.,* **16,** 185– 205.

Sun, D.-Z. and T. Zhang 2006: A Regulatory Effect of ENSO of ENSO on the Time-Mean Thermal Stratification of the Equatorial Upper Ocean, *Res. Lett.,* **33,** L07710, doi:10.1029/2005GL025296.

Sun, D.-Z. 2007: The Role of ENSO in Regulating its Background State. in *Nonlinear Dynamics in Geosciences,* pages 537-555, Edited by J. Elsner and A. Tsonis, Springer New York.

Sun, D.-Z. 2010: The Diabatic and Nonlinear Aspects of El Niño-Southern Oscillation: implications for its Past and Future Behavior. Page 79-104, in

Climate Dynamics: Why Does Climate Vary?, AGU Geophysical Monograph, Edited by D.-Z. Sun and F. Bryan, AGU.

Sun, D.-Z., and Z. Liu 1996: Dynamic ocean–atmosphere coupling: A thermostat for the tropics, *Science,* **272,** 1148–1150.

Sun, D.Z. and R.S. Lindzen, 1994 : A PV view of the zonal mean distribution of temperature and wind in the extratropical troposphere. J. Atmos. Sci., 51, 757-772.

Sun, F. P., J.-Y. Yu, 2009: A 10-15-yr modulation cycle of ENSO intensity. *J. Climate*, **22,** 1718-1735.

Trenberth, K. E., and A. Solomon 1994: The global heat balance: Heat transports in the atmosphere and ocean, *Clim. Dyn.,* **10,** 107–134.

Webster, P. J., and R. Lukas 1992: TOGA COARE: The Coupled Ocean-Atmosphere Response Experiment, *Bull. Am. Meteorol. Soc.,* **73,** 1377-1417.

Zhang, T., D.-Z. Sun, R. Neale, and P. Rasch 2009: An Evaluation of ENSO Asymmetry in the Community Climate System Models: A View from the Subsurface, *J. Climate,* 22, 5933-5961, doi: 10.1175/2009JCLI2933.1.

Figure Legends:

Figure 1: Color schemes used to denote the data from different models and observations. The number of runs for each model and the origin of the countries of the models used are also listed. The dominance of the U.S. in climate modeling is apparent. Only models without the use of flux adjustment are included in this study.

Figure 2 (a): Probability density function (PDF, blue curve) for the climatological annual mean warm pool size. The red vertical line indicates the observed value and the blue vertical line indicates the averaged value of all model runs. The short colored marks on the horizontal axis indicate the ensemble mean values of individual models. (b): Time series for the western Pacific warm-pool size in observations (black) and 19 IPCC models (colors) over the last century. Shown in Fig.2b are the multi-run ensemble mean values smoothed by a cosine bell window with a width of of 49 months. The warm pool is defined as the region where SST is higher than 28ºC. Shown are the results using the data from 1950 to 1999 period, which are considered more reliable. The results based on the data over the entire 20th century are similar to those shown here. Color scheme for identifying models is provided in Figure 1.

Figure 3: The climatology of 28ºC SST in the models (colors) and observations (black). Shown are results for the period 1950 to 1999. Only the results for the ensemble mean of the models are shown in the figure for clarity. Color scheme

for identifying models is provided in Figure 1.

Figure 4: Same as Figure 3, but for all the runs of the same model--the NCAR CCSM3 (a) and GFDL CM2.1 (b). Note that the variability among the different runs is significant in the same model is significant, particularly for the GFDL model, but the variability is small compared to the differences between models and observations.

Figure 5: (a) Same as Figure 2a, but for the mean warm-pool SST; (b) Same as Figure 2b, but for the mean warm-pool SST.

Figure 6: (a) Same as Figure 2a, but for the Maximum SST, (b) Same as Figure 2b, but for the Maximum SST.

Figure 7: The probability density function (PDF) (blue curve) for the skewness of monthly Niño3 SST anomaly. Data used to construct this figure are the same as for Figure 2a. The color scheme for indicating the models is also the same. The red vertical line indicates the value for observations. The vertical blue line is the multi-model ensemble mean. The short color bars on the horizontal axis mark the multi-run ensemble mean values for the individual models.

Figure 8: The frequency distribution of monthly Niño3 SST anomaly. Data and color scheme used in this figure are the same as for Figure 7. Only the ensemble mean of the models are drawn. Color scheme for identifying the models is provided in Figure 1.

Figure 9: Same as Figure 8, but for runs from a single model—the GFDL_CM2_0 (a), GFDL_CM2_1 (b), NCAR CCSM3 (c) and NCAR PCM1 (d).

No.	Data Name	Country	Runs	Color
1	Observations			
2	BCCR−BCM2.0	Norway	1	
3	CNRM−CM3	France	1	
4	CSIRO−Mk3.0	Australia	3	
5	CSIRO−Mk3.5	Australia	3	
6	GFDL−CM2.0	United States	3	
7	GFDL−CM2.1	United States	5	
8	GISS−AOM	United States	2	
9	GISS−EH	United States	5	
10	GISS−ER	United States	9	
11	IAP−FGOALS−g1.0	China	3	
12	INGV−ECHAM4	Italy	1	
13	IPSL−CM4	France	1	
14	MIROC3.2−Hires	Japan	1	
15	MIROC3.2−Medres	Japan	3	
16	MPI−ECHAM5	Germany	3	
17	NCAR−CCSM3.0	United States	2	
18	NCAR−PCM1	United States	3	
19	UKMO−HadCM3	United Kingdom	2	
20	UKMO−HadGEM1	United Kingdom	2	

Figure 1: Color schemes used to denote the data from different models and observations. The number of runs for each model and origin of the countries of the models used are also listed. The dominance of the U.S. in climate modeling is apparent. Most of the models, including those of the U.S., have a very modest number of runs. Note that only models without the use of flux adjustment are included in this study.

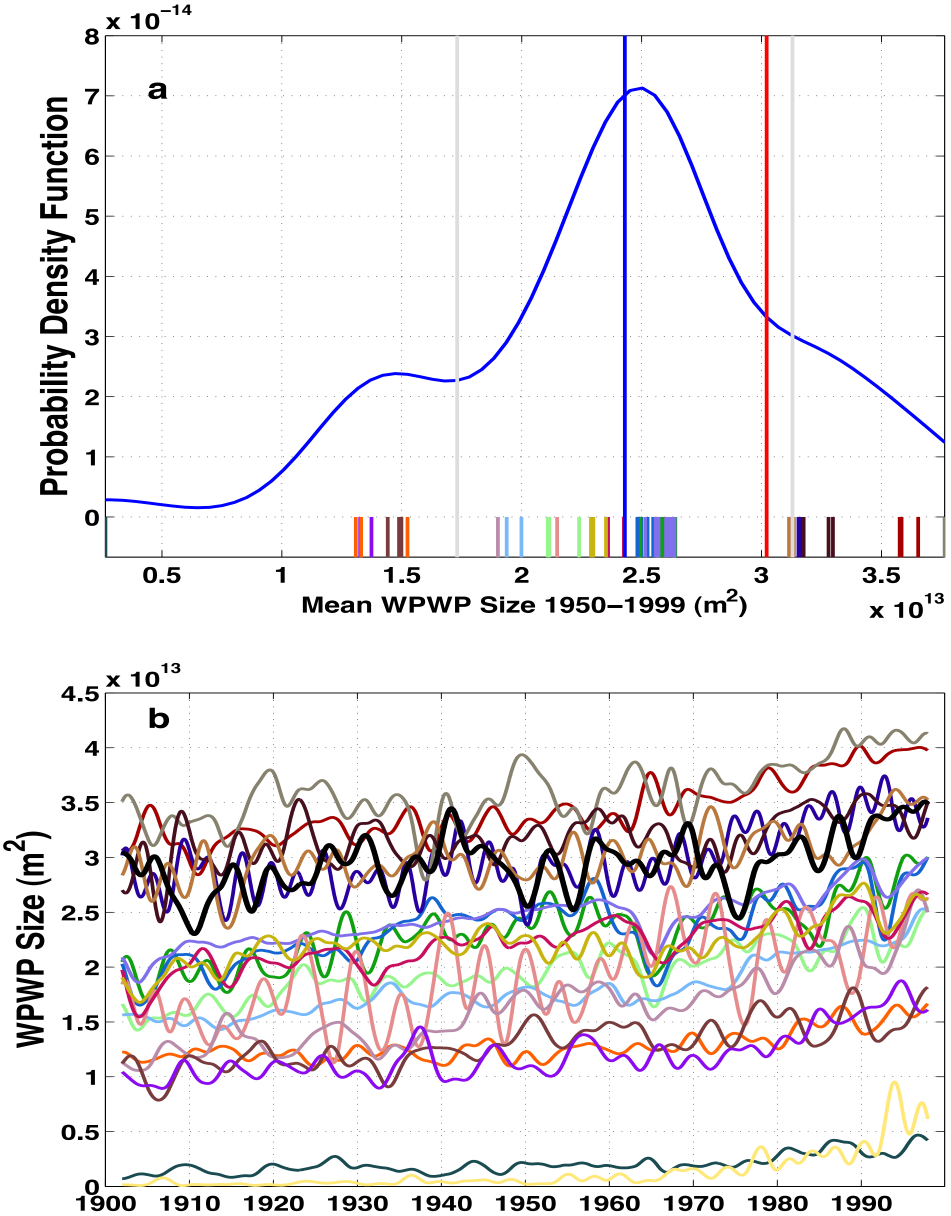

Figure 2 (a): Probability density function (PDF, blue curve) for the climatological annual mean warm pool size. The red vertical line indicates the observed value and the blue vertical line indicates the averaged value of all model runs. The short colored marks on the horizontal axis indicate the ensemble mean values of individual models. (b): Time series for the western Pacific warm-pool size in observations (black) and 19 IPCC models (colors) over the last century. Shown in Figure 2b are the multi-run ensemble mean values smoothed by a cosine bell window with a width of of 49 months. The warm pool is defined as the region where SST is higher than 28ºC. Shown are the results using the data from 1950 to 1999 period, which are considered more reliable. The results based on the data over the entire 20th century are similar to those shown here. Color scheme for identifying models is provided in Figure 1.

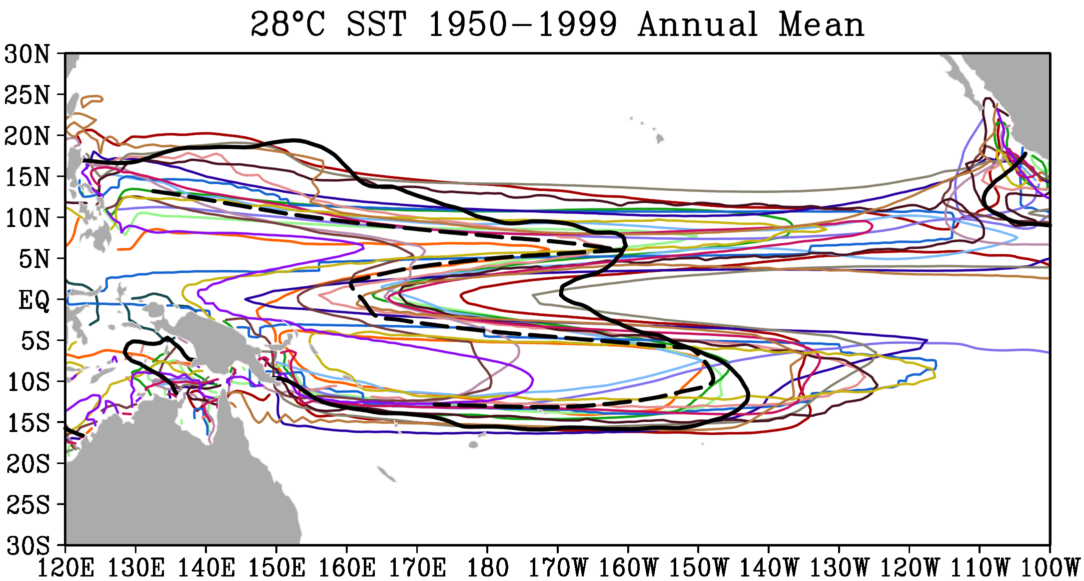

Figure 3: The climatology of 28ºC SST in the models (colors) and observations (black). Shown are results for the period 1950 to 1999. Only the results for the ensemble mean of the models are shown in the figure for clarity. Color scheme for identifying models is provided in Figure 1.

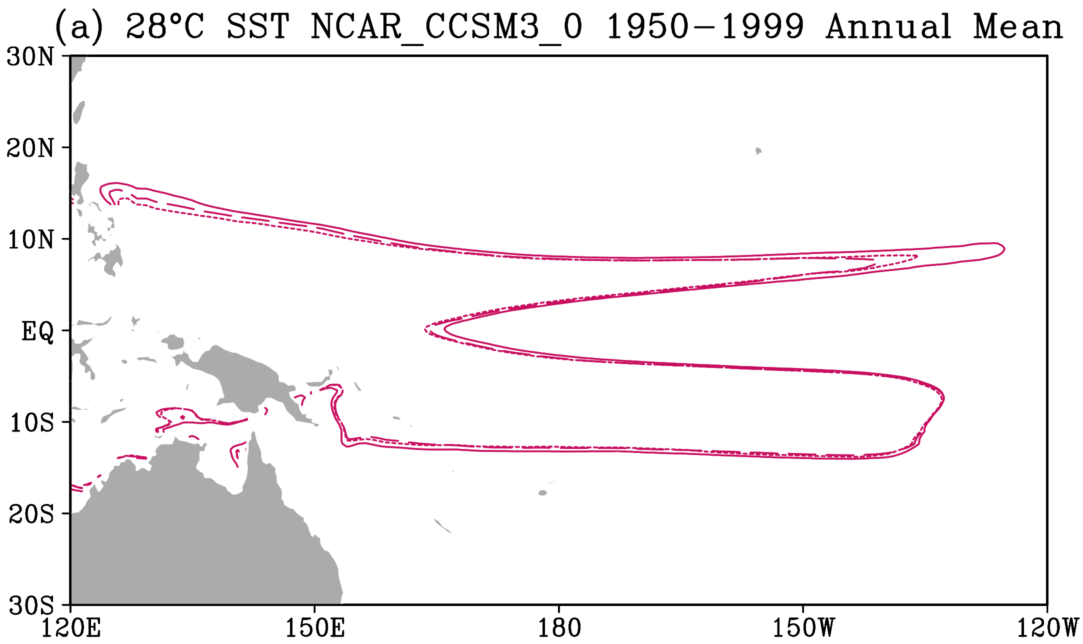

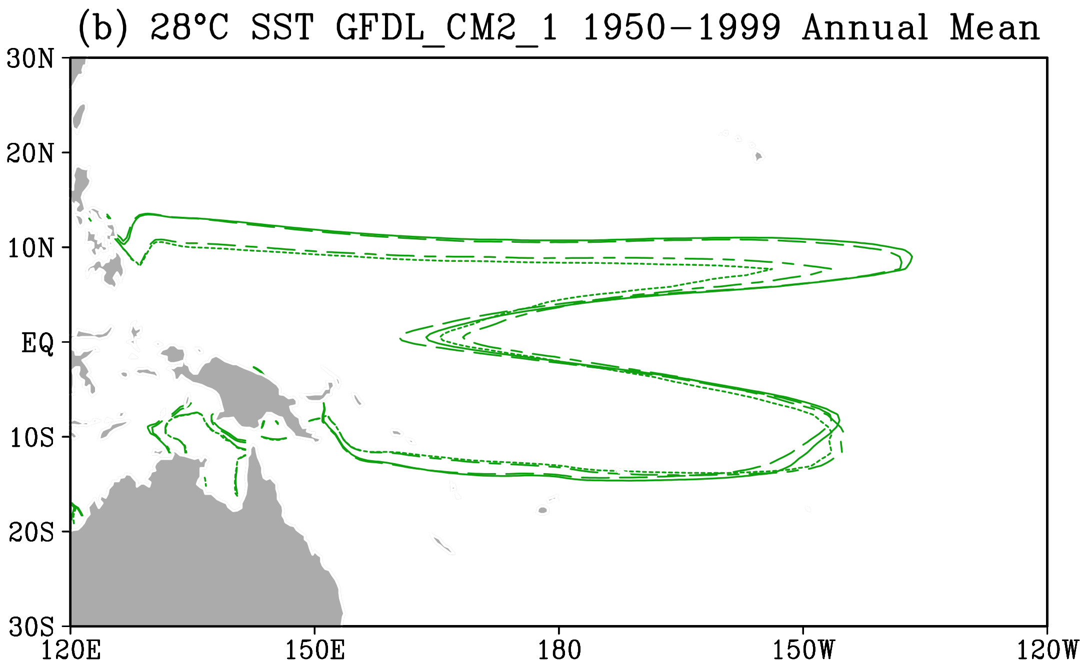

Figure 4: Same as Figure 3, but for all the runs of the same model--the NCAR CCSM3 (a) and GFDL CM2.1 (b). Note that the variability among the different runs is significant in the same model is significant, particularly for the GFDL model, but the variability is small compared to the differences between models and observations.

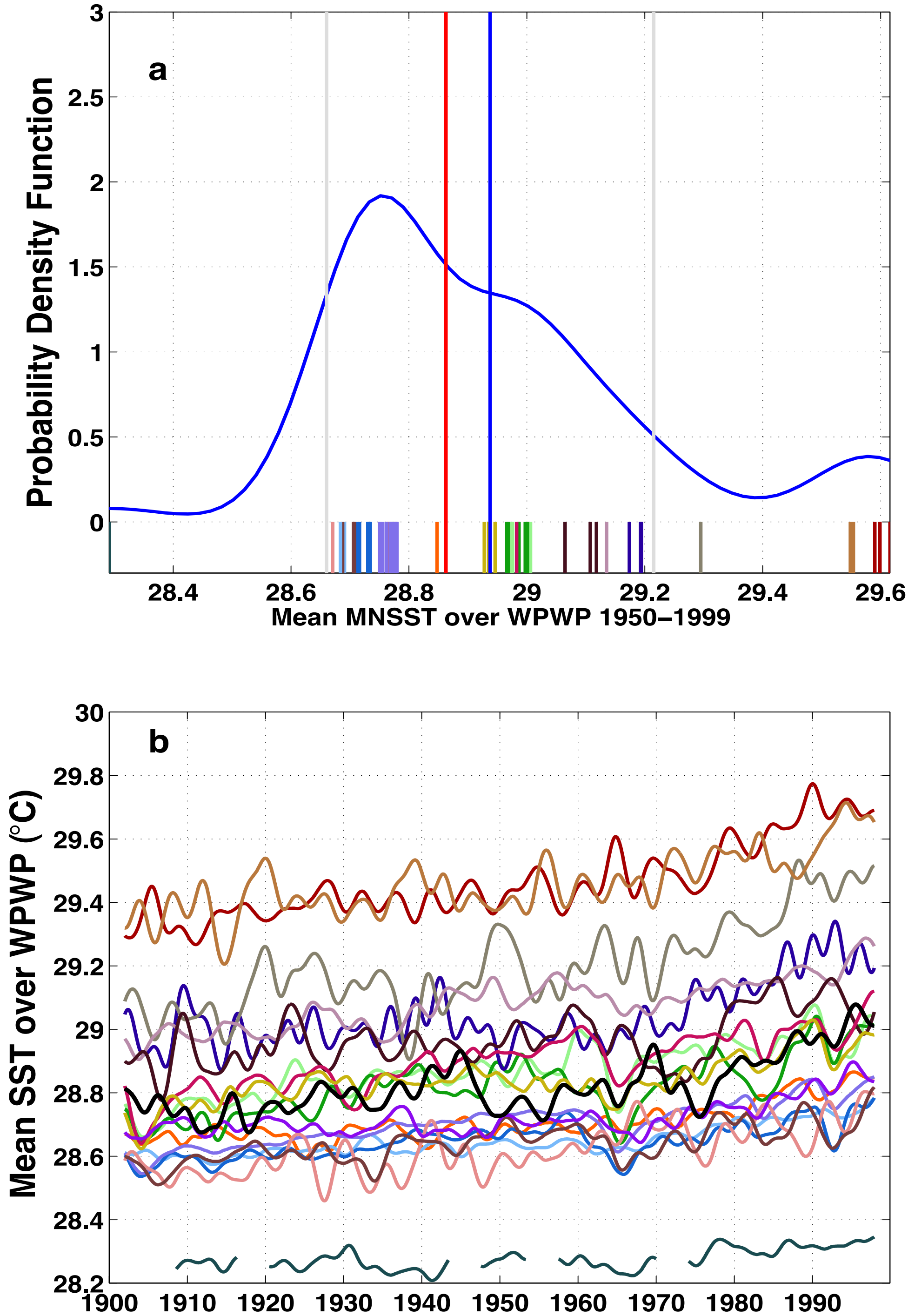

Figure 5: (a) Same as Figure 2a, but for the mean warm-pool SST; (b) Same as Figure 2b, but for the mean warm-pool SST.

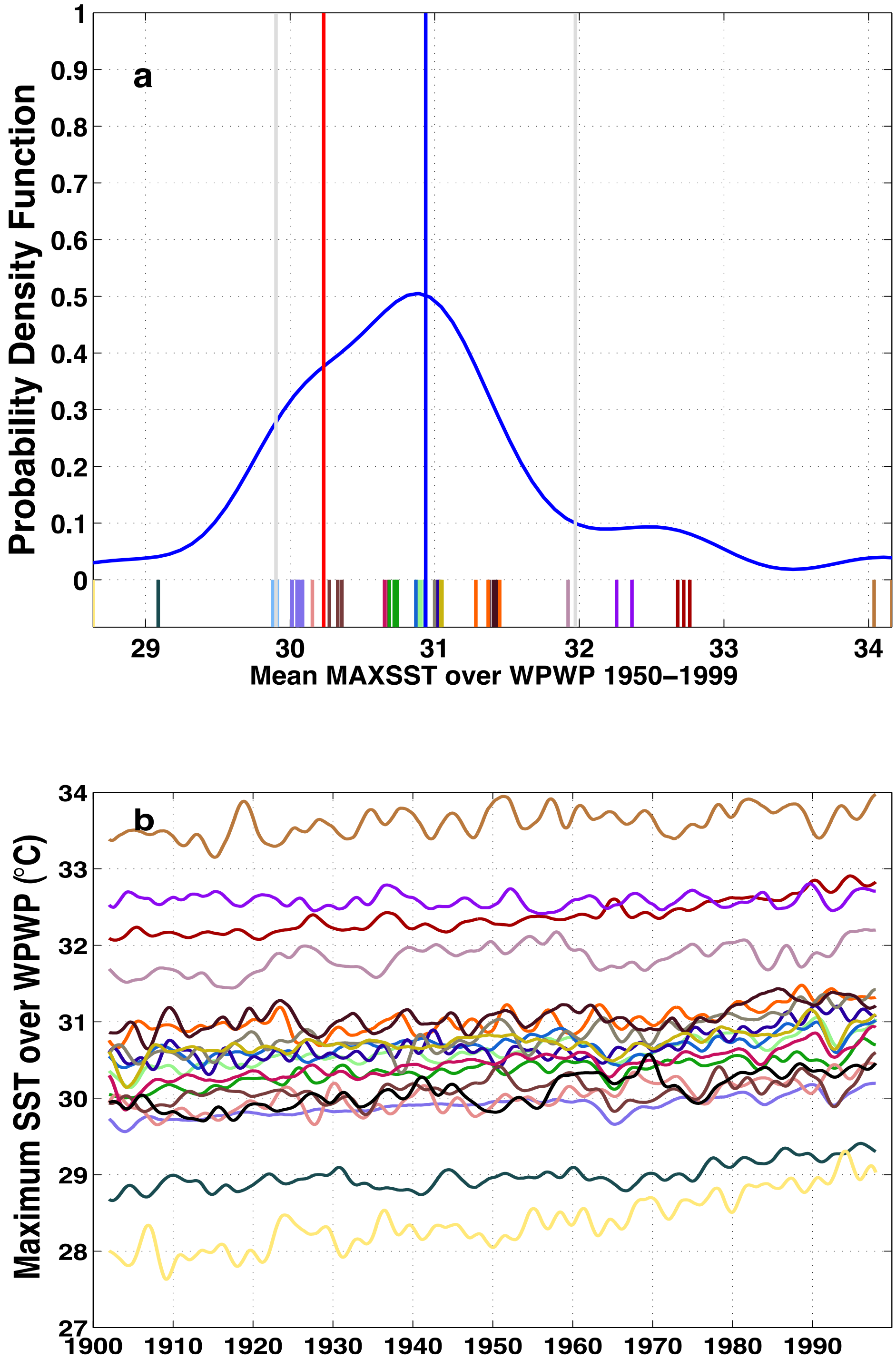

Figure 6: (a) Same as Figure 2a, but for the Maximum SST, (b) Same as Figure 2b, but for the Maximum SST.

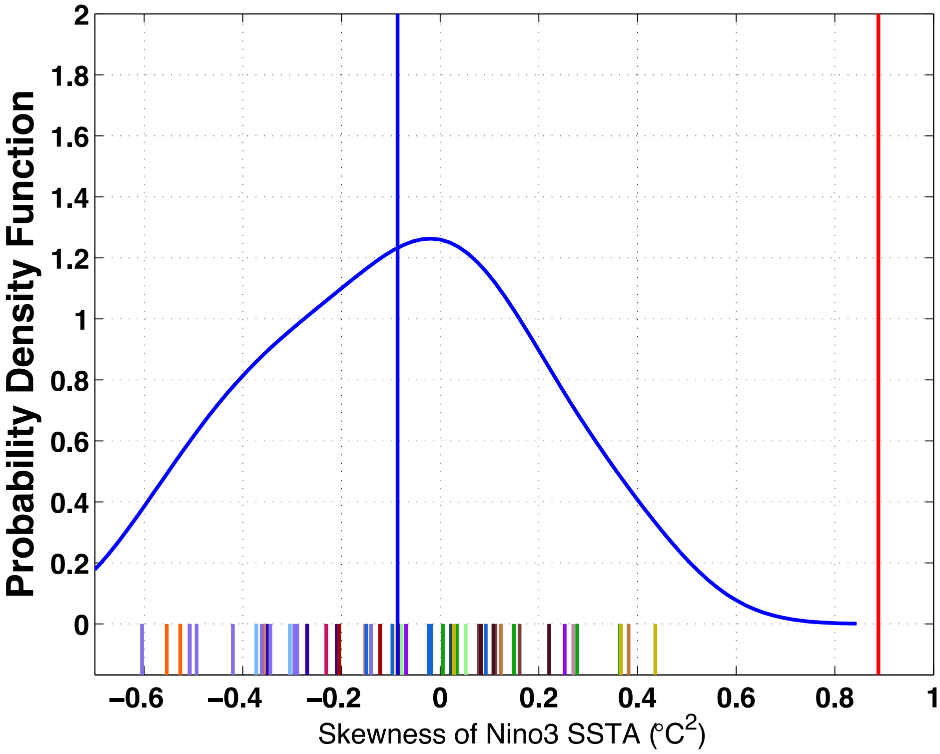

Figure 7: The probability density function (PDF) (blue curve) for the skewness of monthly Niño3 SST anomaly. Data used to construct this figure are the same as for Figure 2a. The color scheme for indicating the models is also the same. The red vertical line indicates the value for observations. The vertical blue line is the multi-model ensemble mean. The short color bars on the horizontal axis mark the multi-run ensemble mean values for the individual models.

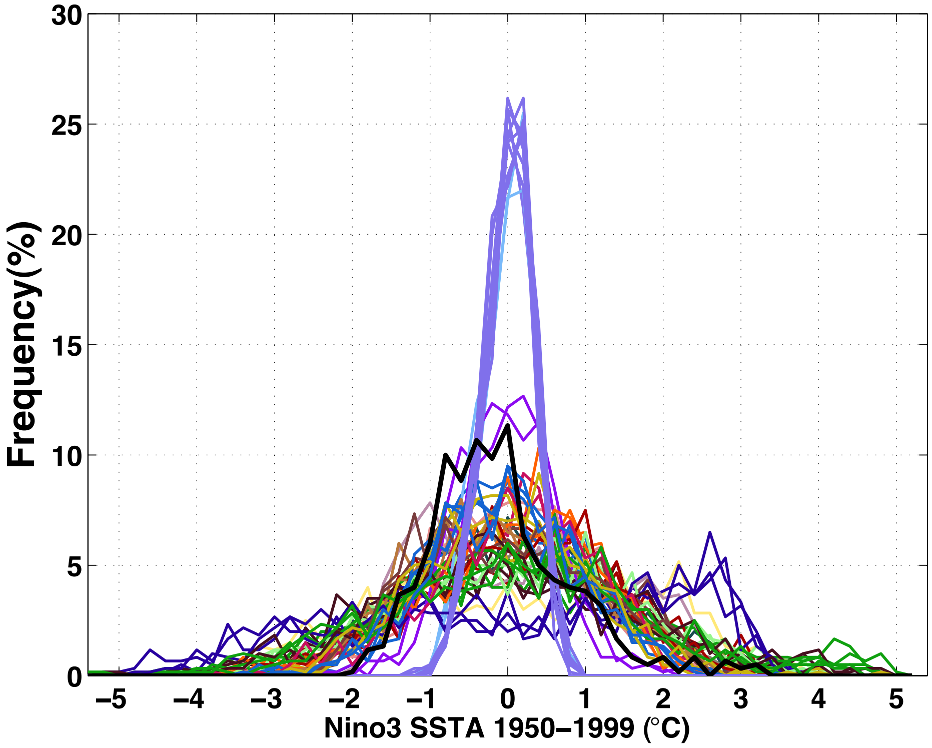

Figure 8: The frequency distribution of monthly Niño3 SST anomaly. Data and color scheme used in this figure are the same as for Figure 7. Only the ensemble mean of the models are drawn. Color scheme for identifying the models is provided in Figure 1.

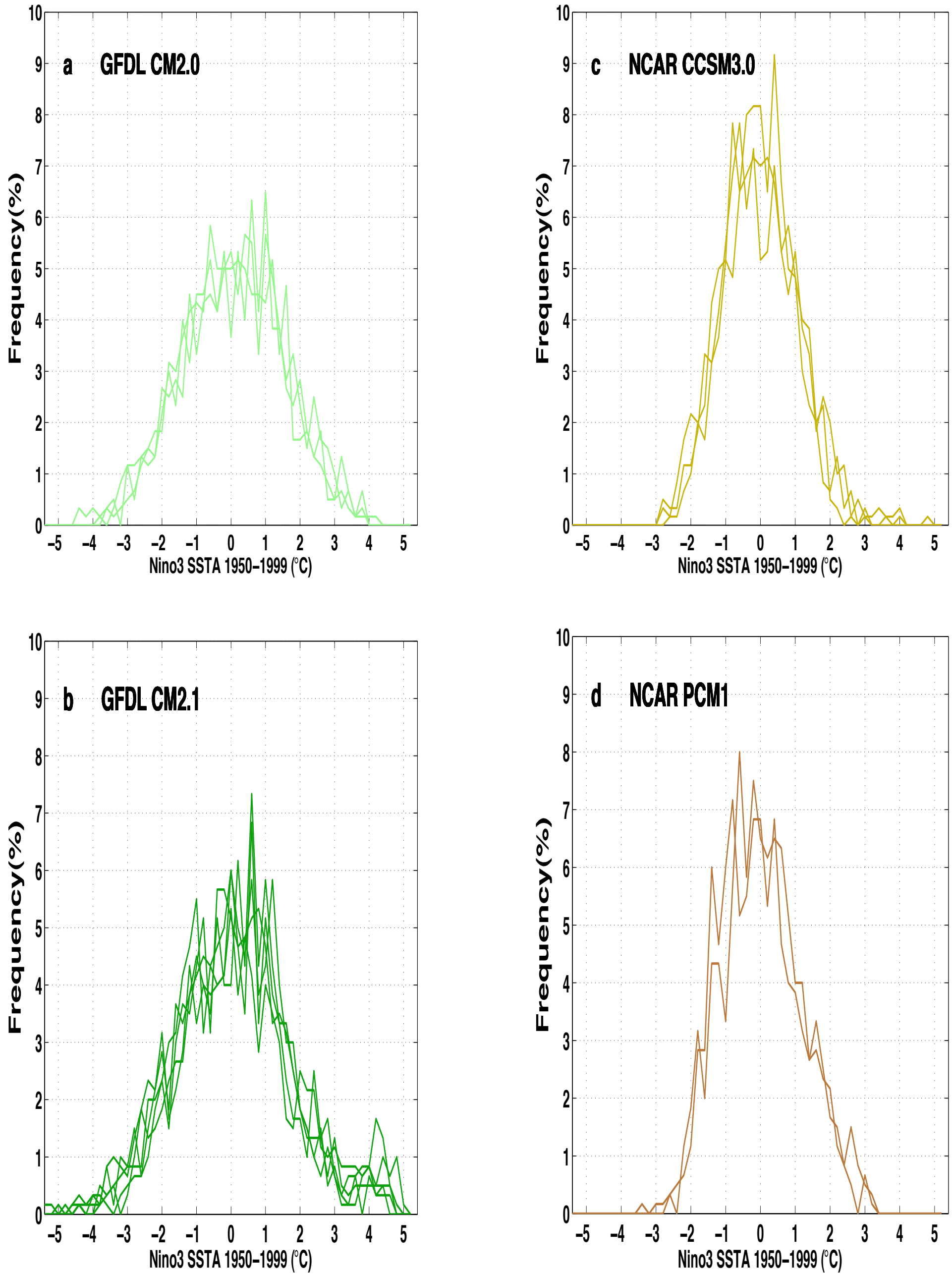

Figure 9: Same as Figure 8, but for runs from a single model—the GFDL_CM2_0 (a), GFDL_CM2_1 (b), NCAR CCSM3 (c) and NCAR PCM1 (d).